Single-molecule analysis of DNA-protein complexes using nanopores

Breton Hornblower[1,2], Amy Coombs[1], Richard D Whitaker[3,5], Anatoly Kolomeisky[4], Stephen J Picone[3,5], Amit Meller[2] & Mark Akeson[1]

We present a method for rapid measurement of DNA-protein interactions using voltage-driven threading of single DNA molecules through a protein nanopore. Electrical force applied to individual ssDNA-exonuclease I complexes pulls the two molecules apart, while ion current probes the dissociation rate of the complex. Nanopore force spectroscopy (NFS) reveals energy barriers affecting complex dissociation. This method can be applied to other nucleic acid–protein complexes, using protein or solid-state nanopore devices.

The strength and specificity of DNA-protein interactions are typically quantified using bulk biochemical and biophysical methods. Although these methods yield information about the behavior of populations of molecules, they are limited in their ability to detect variation within populations and detailed features of binding kinetics. In contrast, single-molecule measurements can reveal information masked by ensemble averaging in bulk, such as bond strength and the presence of short-lived intermediate states[1]. To obtain meaningful statistics with single-molecule approaches, hundreds of copies of the same complex must be analyzed. This often represents a challenge for methods such as atomic force microscopy and optical tweezers that require specific immobilization of the molecules to the force probe at one end, and to a reference surface at its other end[1].

We present a method for single-molecule analysis of DNA-protein interactions using NFS that can be used to analyze hundreds of molecules in minutes. Instead of surface immobilization, nanopores are used to capture and manipulate DNA-protein complexes. This allows rapid determination of association and dissociation rates by combining measurements under equilibrium and nonequilibrium conditions.

A single α–hemolysin (α-HL) nanopore is inserted into a planar lipid bilayer, resulting in a steady open-channel ionic current (**Fig. 1a**). Passage of short ssDNA molecules through the pore results in brief, measurable blockades of the current (**Fig. 1b**). The electrical field, temperature and ssDNA length can be adjusted to yield a translocation distribution time around 100 μs (ref. 2). Binding of streptavidin to biotinylated ssDNA allows capture but not translocation of the polynucleotide because the protein bound at one end is larger than the pore diameter[3]. This results in very long ($\gg$1 s) blockades that require voltage reversal to clear. By comparison, weaker DNA-protein complexes are expected to dissociate in the pore under applied voltage and thus result in modest, yet measurable increases in translocation time relative to ssDNA alone (from microseconds to milliseconds). This increase in translocation time can be discerned setting the stage for nanopore-based

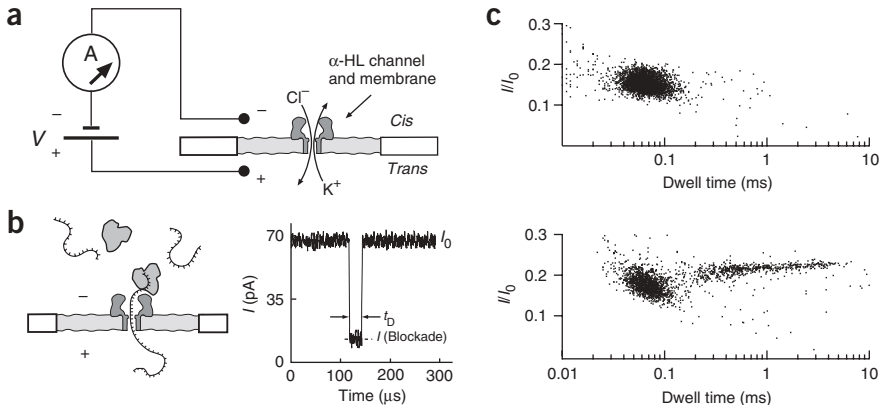

Figure 1 | Detecting ssDNA-ExoI complexes using a nanopore. (**a**) Schematic of the experimental setup[14,15]. Voltage is applied across a single α-HL channel inserted in an ~20-μm-diameter bilayer (*trans* side positive). Current through the open pore is carried by K^+ and Cl^- ions (1 M bulk concentration). (**b**) I_0 is the open channel current in the absence of DNA. Capture of ssDNA or enzyme-bound ssDNA results in partial blockade of the current. We denote the average current level and the translocation dwell time during each individual blockade as I and t_D, respectively. (**c**) Dwell time versus normalized event amplitude for ssDNA alone (top) and for equimolar ssDNA and ExoI (bottom). Each point represents the event amplitude (I/I_0) and its dwell time, at 180 mV applied potential. In the bottom panel, the cluster on the left with the tight dwell-time distribution represents free oligonucleotide translocations, and the population on the right, with the broader time distribution, represents translocations that occur after capture of ssDNA-ExoI complexes.

[1]Departments of Chemistry & Biomolecular Engineering, MS SOE2, University of California, Santa Cruz, California 95064, USA. [2]Departments of Biomedical Engineering & Physics, Boston University, 44 Cummington St., Boston, Massachusetts 02215, USA. [3]New England Biolabs, 240 County Road, Ipswich, Massachusetts 01938, USA. [4]Department of Chemistry, MS60 Rice University, Houston, Texas 77005, USA. [5]Present address: Enzymatics, 100 Cummings Center, Suite 336H, Beverly, Massachusetts 01915, USA. Correspondence should be addressed to M.A. (makeson@chemistry.ucsc.edu) or A.M. (ameller@bu.edu).

RECEIVED 1 SEPTEMBER 2006; ACCEPTED 29 JANUARY 2007; PUBLISHED ONLINE 4 MARCH 2007; DOI:10.1038/NMETH1021

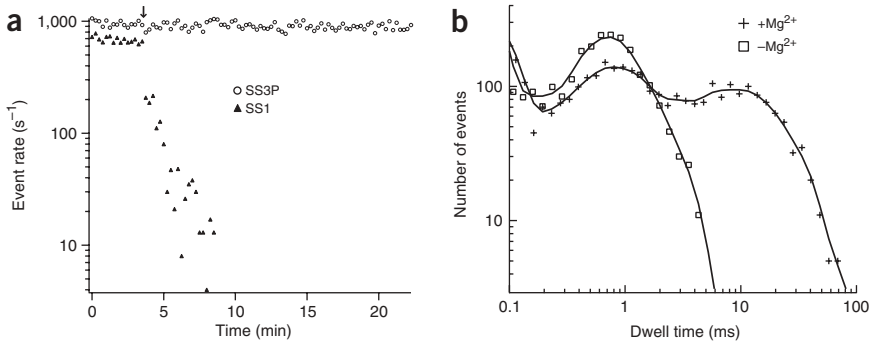

Figure 2 | Monitoring ExoI digestion of DNA using a nanopore. (**a**) The DNA capture rate in the nanopore as a function of time. After addition of 5 mM Mg^{2+} (arrow), the event rate sharply declines for SS1 (3′-OH end). In contrast, the event rate is maintained for SS3P (3′-phosphorylated end). (**b**) Translocation-time distributions for complexes of SS3P-ExoI in the presence and absence of 5 mM Mg^{2+}. Lines represent binomial smoothing of the data.

analysis of biologically relevant interactions between nucleic acids and proteins.

We illustrate this approach using the interaction of ssDNA with Exonuclease I (ExoI; see **Supplementary Methods** online). Each translocation of DNA through the α-HL channel is characterized by two parameters: (i) the averaged normalized blocked current, $I_B = I/I_0$, where I is the measured blockade conductance and I_0 is the open-pore current, and (ii) t_D, the translocation dwell time. We plotted I_B versus t_D values for nearly 2,000 translocation events at 180 mV potential for a ssDNA 64-mer (SS1) in the absence of ExoI (**Fig. 1c**). We observed a well-defined distribution, with a current peak at 16% of the open-pore current ($I_B = 0.16$) and a characteristic (most probable) translocation time, t_p of 66 ± 10 μs. Upon addition of ExoI (without Mg^{2+}), an additional broadly distributed population of events appeared with $I_B = \sim 0.22$ and $t_p = 380 \pm 50$ μs (**Fig. 1c**). Backward escape of ssDNA molecules into the *cis* compartment would result in very long dwell times ($\sim 10^2$ s)[4,5] and therefore cannot explain this observation. Thus the new population of translocation events was due to capture and retention of the ssDNA-ExoI complex until it dissociated in the nanopore. The relative number of ssDNA translocations in the presence or absence of ExoI can be used to solve for the equilibrium dissociation constant of the ssDNA-ExoI binding reaction (**Supplementary Note** online) giving an equilibrium dissociation constant (K_D) of $4.8 \times 10^{-7} \pm 1.7 \times 10^{-7}$ M.

The 3′-exonucleolytic activity of ExoI is dependent upon Mg^{2+} ions, which form the enzyme's catalytic site when coordinated by essential carboxylate residues[6]. Bulk assays based on fluorescently labeled ssDNA (**Supplementary Fig. 1** online) showed that Mg^{2+}-dependent catalytic activity was fully retained under conditions used for the nanopore experiments. Nanopore experiments accurately reported this catalytic activity as an abrupt decrease in translocation-event frequency after addition of 5 mM Mg^{2+} to SS1-ExoI complexes (**Fig. 2a**). In contrast, event frequency for a 3′-phosphorylated DNA oligomer (SS3P) remained stable after Mg^{2+} addition (**Fig. 2a**), consistent with previous biochemical studies showing that this modification inhibits hydrolysis by ExoI (ref. 7). Moreover, the addition of Mg^{2+} to SS3P-ExoI complexes revealed a new subpopulation of translocation events (**Fig. 2b**), characterized by a longer dwell time ($t_p = \sim 10$ ms), indicative of tighter DNA-ExoI binding.

We probed the dissociation kinetics of the ssDNA-ExoI complexes under time-varying force using NFS. Similar to conventional dynamic force spectroscopy, NFS reveals information about energy barriers affecting molecular dissociation. This technique recently has been used to measure the unzipping kinetics of DNA hairpins[4,8]. It resembles constant voltage nanopore unzipping of duplex DNA[4,9], but NFS automatically ramps the applied voltage upon capture of a molecule. When bonds are ruptured under steady

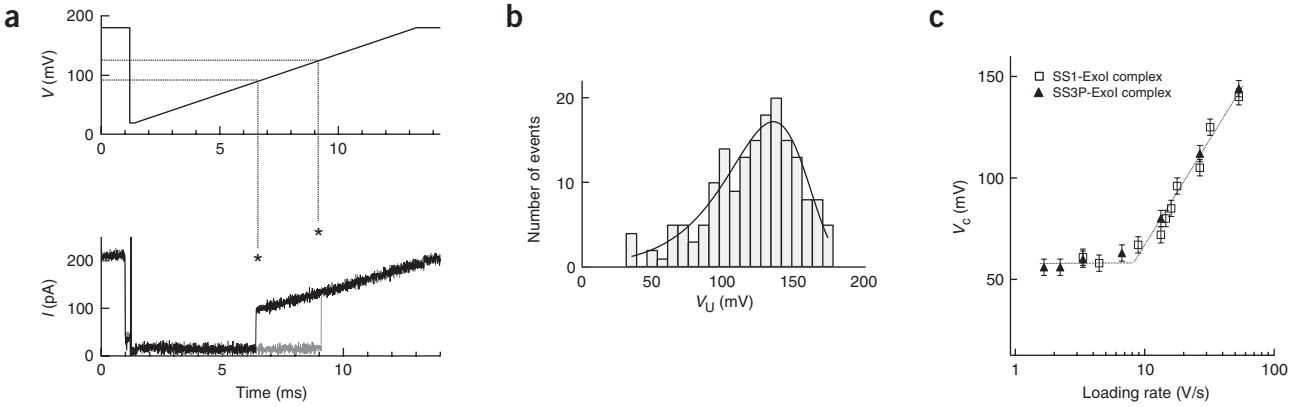

Figure 3 | NFS of DNA-protein complexes. (**a**) Current and voltage profiles during two typical events in a nanopore voltage-ramp force spectroscopy experiment. Plotted are the time-dependent voltage applied to each individual complex (top), and the measured pore current (bottom). Dissociation of the complexes results in an abrupt rise of the current (asterisks) to the open-pore level. Dashed lines are shown to indicate the voltage where dissociation occurred for each of the two events (V_U). (**b**) A typical distribution of dissociation voltage, measured at a loading rate of 30 V/s. (**c**) Plots of log loading rate versus V_C for SS3P-ExoI and SS1-ExoI complexes. The V_C for each loading rate was determined to be the maximum of the histogram of at least 500 dissociation events, such as those shown in **Figure 3b**. Error bars represent the width of the bins in each histogram.

ramps of force, the rupture force depends on the loading rate, $\dot{v}$ (force/time or voltage/time)[1]. We analyzed the dependence of the most probable rupture voltage, V_c, on $\dot{v}$ for ssDNA-ExoI complexes by measuring the distributions of rupture voltages over a wide range of $\dot{v}$ values. For each loading rate value, $\dot{v}$, we collected at least 500 unbinding events (**Fig. 3a**). The voltage level at which complex dissociation occurs (V_U) was marked by an abrupt rise in the current. A typical distribution of V_U values at $\dot{v} = 30$ V/s (**Fig. 3b**) displays a clear peak defined as V_C (and is fitted by equation 4 in **Supplementary Note**).

We repeated these measurements for $\dot{v}$ values ranging from 1.6 V/s to 53.3 V/s, obtaining the voltage-induced dissociation distributions in each case. When V_C was plotted as a function of log $\dot{v}$ (**Fig. 3c**) we observed two regimes for both the SS1-ExoI complex and the SS3P-ExoI complex. At high ramp values ($\dot{v} > 8$ V/s), V_C scaled with log $\dot{v}$, but at lower ramp values ($\dot{v} < 8$ V/s) the curve reached a plateau at a voltage of ~60 mV. The logarithmic scaling of the critical force (voltage) with the loading rate has previously been observed for other bimolecular systems using conventional force spectroscopy[1] and for DNA hairpins using NFS[4,8]. Application of time varying force (or voltage) gradually lowers energy barriers and thus destabilizes the captured complex[1,10–12].

A model developed independently of these experiments predicts the two regimes if rebinding is allowed (**Supplementary Note** online). That is, it predicts a logarithmic scaling at high $\dot{v}$,

$$V_C = \frac{k_B T}{q\theta} \log\left(\frac{\dot{v} q \theta}{k_d k_B T}\right)$$

and a region where the critical voltage is independent of $\dot{v}$ at very low loading rates,

$$V_C = k_B T / q \log({K_D}^{-1}).$$

In these equations k_BT is the thermal energy, q is a constant in units of charge, θ is a dimensionless constant describing the shape of the barrier, k_d is the bulk off-rate constant, and K_D is the equilibrium dissociation constant.

This model not only predicts the two regimes we observed (**Fig. 3c**), but it can be used to calculate the kinetic binding constants of the ssDNA-ExoI interaction. When we substituted the measured value of K_D, the value of V_C at the plateau regime and the slope of the logarithmic regime into the two equations above, they together gave $k_d = 37 \pm 6$ s^{-1}, $\theta = 0.10 \pm 0.02$ and $q = (6.1 \pm 1.1)e$. Once k_d has been determined, the measured value of K_D can be used to calculate the association rate constant, $k_a = k_d/K_D = (1.0 \pm 0.3) \times 10^8$ s^{-1}M^{-1}.

The association rate constant k_a obtained from our data is approximately equal to the theoretical diffusion limit of the protein, and is consistent with previous studies that suggest a lower limit for k_a on the order of 10^7 s^{-1}M^{-1} for DNA-ExoI interaction[13]. Thus the two-regime curve for V_C versus log $\dot{v}$ obtained by NFS, along with K_D (also measured using the nanopore) revealed details of ExoI-DNA binding kinetics that would be otherwise difficult to detect, demonstrating the power of this method for the analysis of nucleic acid-protein interactions.

Note: Supplementary information is available on the Nature Methods website.

ACKNOWLEDGMENTS

We thank D. Branton, D. Deamer and A. Marziali for thoughtful critiques of early drafts of this manuscript. K. Lieberman edited the final draft and provided important advice on presentation of our results. S. Benner and R. Abu-Shumays provided technical assistance. This work was supported by US National Human Genome Research Institute Grant HG003703 (M.A.), National Institute of General Medical Sciences Grant GM075893 (A.M.), National Science Foundation Grant NIRT-26384 (A.M.) and Human Frontier Science Program Award RGP0036/2005 (A.M.). Concentrated stocks of Exonuclease I were a gift from New England Biolabs.

AUTHOR CONTRIBUTIONS

B.H. performed the majority of nanopore experiments and wrote the first draft of the manuscript; A.C. performed nanopore experiments in Santa Cruz; R.D.W. and S.J.P. contributed ExoI purification and ExoI biochemical assays; A.K. contributed theoretical models; A.M. and M.A. directed the research and are responsible for the overall quality of the work.

COMPETING INTERESTS STATEMENT

The authors declare competing financial interests: details accompany the full-text HTML version of the paper at www.nature.com/naturemethods.

Published online at http://www.nature.com/naturemethods/
Reprints and permissions information is available online at http://npg.nature.com/reprintsandpermissions

1. Evans, E. *Annu. Rev. Biophys. Biomol. Struct.* **30**, 105–128 (2001).
2. Meller, A., Nivon, L. & Branton, D. *Phys. Rev. Lett.* **86**, 3435–3438 (2001).
3. Kasianowicz, J.J., Henrickson, S.E., Weetall, H.H. & Robertson, B. *Anal. Chem.* **73**, 2268–2272 (2001).
4. Mathe, J., Visram, H., Viasnoff, V., Rabin, Y. & Meller, A. *Biophys. J.* **87**, 3205–3212 (2004).
5. Bates, M., Burns, M. & Meller, A. *Biophys. J.* **84**, 2366–2372 (2003).
6. Breyer, W.A. & Matthews, B.W. *Nat. Struct. Biol.* **7**, 1125–1128 (2000).
7. Lehman, I.R. & Nussbaum, A.L. *J. Biol. Chem.* **239**, 2628–2636 (1964).
8. Mathe, J., Arinstein, A., Rabin, Y. & Meller, A. *Europhys. Lett.* **73**, 128–134 (2006).
9. Nakane, J., Wiggin, M. & Marziali, A. *Biophys. J.* **87**, 615–621 (2004).
10. Dudko, O.K., Filippov, A.E., Klafter, J. & Urbakh, M. *Proc. Natl. Acad. Sci. USA* **100**, 11378–11381 (2003).
11. Hummer, G. & Szabo, A. *Biophys. J.* **85**, 5–15 (2003).
12. Dudko, O.K., Hummer, G. & Szabo, A. *Phys. Rev. Lett.* **96**, 108101 (2006).
13. Brody, R.S., Doherty, K.G. & Zimmerman, P.D. *J. Biol. Chem.* **261**, 7136–7143 (1986).
14. Mathe, J., Aksimentiev, A., Nelson, D.R., Schulten, K. & Meller, A. *Proc. Natl. Acad. Sci. USA* **102**, 12377–12382 (2005).
15. Akeson, M., Branton, D., Kasianowicz, J.J., Brandin, E. & Deamer, D.W. *Biophys. J.* **77**, 3227–3233 (1999).